Hindawi
Advances in Civil Engineering
Volume 2019, Article ID 6074781, 17 pages
https://doi.org/10.1155/2019/6074781

*Research Article*

# Accurate Method for Picking Up the First Arrival Time of Microseismic Signals Based on Entropy Theory

**Bao-xin Jia**[1,2] **Ao Sun**[1] **Yi-shan Pan**[3] **Hao Chen**[1] **and Feng-pu Liu**[1]

[1]*School of Civil Engineering, Liaoning Technical University, Fuxin 123000, China*
[2]*Institute of Geology, China Earthquake Administration, Beijing 100000, China*
[3]*Liaoning University, Shenyang 110036, China*

Correspondence should be addressed to Bao-xin Jia; 13941855200@126.com

Received 25 August 2018; Revised 25 January 2019; Accepted 11 February 2019; Published 18 March 2019

Academic Editor: Venu G. M. Annamdas



The entropy method describes the change in the signal state from a macroscopic angle and weakens the interference generated by random noise. From the angle of chaos, which describes the first arrival of microseismic signals, it predicts the trend of noise entropy based on the grey theory. The results indicate that the entropy method is sensitive to amplitude, frequency, and seismic phase changes. Compared with traditional methods, the entropy method has better noise immunity. In terms of the influence of the pickup parameter on the resulting error, the entropy method demonstrated the best result and produces the smallest error.

## 1. Introduction

In China, coal is a basic energy resource and has an irreplaceable role in the energy infrastructure. With the rapid development of the Chinese economy, the consumption of coal has significantly increased. The availability of coal in shallow areas has gradually dried up, which has changed the coal industry from shallow to deep mining. Owing to the continuous mining of coal, an increasing number of disasters have occurred [1–4]. Under this particular background, research into microseismic monitoring technology has significantly increased [5–8]. The location of the hypocenter can be realized using a microseismic technique. To locate the microseismic source, it is necessary to pick up the first arrival time of the wave, and therefore how to overcome the presence of noise and precisely pick up the first arrival time is an urgent problem.

Many scholars have conducted research on the picking up the microseismic signal's first arrival, and many different research methods have been put forward. The time window energy ratio method is more intuitive and less computational and is therefore widely used in engineering fields. However, because a static partition window is applied, the energy ratio of the window may not be the largest at the first arrival time, and it is therefore easy to incorrectly pick up the first arrival of a signal [9]. The AIC [10] is a different steady-state process for the front and back recording of the initial arrival time. It uses the autoregressive AR-AIC method to apply the first arrival discriminant of the microseismic moments. Although the AIC used for the energy ratio method is more accurate for picking up the signal of the first arrival, it has the disadvantage of a large number of computations. Based on the time window energy ratio and AIC method, Zhang et al. [11] proposed a new method for accurately picking up the initial arrival time of microseismic waves. This method synthesizes the advantages of the two methods to a certain extent. Allen [12, 13] constructed a characteristic function based on the traditional time window energy ratio method. This feature function can amplify the first arrival time of the signal and accurately pick it up. Liu et al. [14] synthesized the time window energy ratio method and the AIC method, and based on higher order statistics, skewness, and kurtosis of the PAIS/K method, they proposed the moving time window kurtosis as a fast method and an improved kurtosis pickup of the first arrival method. According to the fractal theory, Jia et al. [15] use the Hausdorff dimension calculation method. The first arrival time of the signal is picked up from the three-dimensional

fractal angle for the first time. Aiming at the inherent characteristics of microseismic signals, Jia et al. [16] proposed a new method for automatically picking up the seismic phase of the first arrival, which is based on a combination of a Hilbert–Huang transform (HHT) and the AIC. Because the HHT is a new theory, its physical meaning is not yet clear, and the results are extremely random, requiring further study. Tan et al. [17] synthesized seismic signals and environmental noises in terms of the differences in amplitude, polarization, and statistical characteristics proposed by the SLPEA algorithm. This method is a combination of other current methods and has a function built in to judge the first arrival of the signals. Scholars have conducted a number of studies on the pickup of the first arrival of vibrations, although most methods require setting a fixed critical value. The selection of this critical value is based more on experience, whereas monitoring the environment and vibration waveform is also related to its selection. In general, the same fixed critical value cannot meet the precision requirements of different vibration types and different signal-to-noise ratios. The selection of the critical value has a significant influence on the pickup accuracy, and the selection of the appropriate critical value is the main reason for requiring an accurate pickup.

In this paper, a new accurate pickup method, called the entropy method, is proposed for determining the characteristics of microseismic waves. At present, the entropy method has been preliminarily applied in many disciplines, such as the detection of lesion signals in medicine [18, 19], the analysis of seismic activity [20, 21], and rock mechanics [22]. The method proposed in this paper introduces the entropy theory through artificial partitions, which describe the first arrival of a wave from the angle of chaos, and predicts the trend of noise entropy based on the grey theory. The new method overcomes the shortcomings of the traditional method in the setting of a fixed critical value and achieves a more accurate pickup of the first arrival.

## 2. Theoretical Basis

*2.1. Entropy.* Information theory refers to the basic philosophical view of the interrelationship and interaction between things and deeply analyzes the relationship between information and a material. Entropy is an important aspect of information theory. Entropy is a key metric of information and usually refers to the average number of bits in a piece of information that needs to be transmitted or stored. Entropy measures the uncertainty of predictive random variables. The greater the uncertainty, the larger the amount of entropy [23]. Entropy is an important part of information theory. The entropy value can describe the uncertainty and varying degree of a random series used in information theory. In a set, the entropy value can also describe the degree of irregularity, that is, the degree of association among the elements. If the degree of variation of a sequence is large or the degree of association between the elements of a set is smaller, the entropy value will be larger. In contrast, the entropy value is smaller. Above all, the entropy value is widely used in describing the randomness of data, the order of structures, and the disorder of events.

Here, $X$ represents a situation in which an event is likely to occur and $p(x)$ is the probability of the occurrence of each event, namely,

$$\begin{bmatrix} X \\ p(x) \end{bmatrix} = \begin{bmatrix} x_1 & x_2 & \cdots & x_n & x_{n+1} \\ p_1 & p_2 & \cdots & p_n & p_{n+1} \end{bmatrix}, \quad p_i \geq 0 \text{ and } \sum_{i=1}^{n+1} p_i = 1. \tag{1}$$

The negative value of the logarithm of an event probability is defined as the amount of information for that event, that is, $I(xi) = -\log pi$. $I(xi)$ represents the amount of information that one $X_i$ contains when a message source sends out a signal. Therefore, when sending different information, $I(xi)$ is not the same. This cannot be used as a mathematical quantity to describe a signal. To avoid this situation, Shannon proposed the mean of information, which is the use of entropy to describe an entire event. The existence formula is as follows:

$$H(X) = E\left[I(x_i)\right] = -\sum p_i \log p_i. \tag{2}$$

*2.2. Grey Theory*

*2.2.1. Theoretical Basis.* Professor Deng Julong proposed the grey theory in 1982. He believed that all random processes change within a certain range and are random variables corresponding to time. Although data have a certain amount of randomness, there must be some connection between them. The traditional research method determines the statistical rules by collecting a large number of samples. The grey theory is used to sort the samples and make them show a certain rule, allowing a prediction to be made.

*2.2.2. Realization of Grey Forecast.* Let the primitive numbers be

$$X^0 = \left\{x^{(0)}(1), x^{(0)}(2), \ldots, x^{(0)}(n)\right\}. \tag{3}$$

One way to find a rule is to accumulate the raw data, the resulting sequence of which is called the 1-AGO sequence. This superposition or decrease by degree will lead irregular raw data to show a certain regularity:

$$X^{(1)} = \left\{x^{(1)}(1), x^{(1)}(2), \ldots, x^{(1)}(n)\right\}. \tag{4}$$

In the formula below, $k = 1, 2 \ldots n$.

The smoothness detection is as follows:

$$\rho(t) = \frac{X^{(0)}(t)}{X^{(1)}(t-1)} < 0.5. \tag{5}$$

To select the model, for the transformed sequence $X^{(1)}$ that establishes a differential equation model is the GM$(n, n)$ model. The model represents differential equations of $n$ order and $n$ variables.

We call sequence $Z^{(1)}$, which is the generated mean sequence of consecutive neighbours of sequence $X^{(1)}$, that is,

$$Z^{(1)} = \left\{z^{(1)}(1), z^{(1)}(2), \ldots, z^{(1)}(n)\right\}. \quad (6)$$

In formula (6), $z^{(1)}(k) = 0.5x^{(1)}(k) + 0.5x^{(1)}(k-1)$.

The definition type of GM(1, 1), that is, the grey differential equation of GM(1, 1) is as follows:

$$x^{(0)}(k) + az^{(1)}(k) = b, \quad (7)$$

where $a$ is called the development the coefficient and $b$ is the grey function. Set $\hat{\alpha}$ as the parameter vector to be estimated, that is, $\hat{\alpha} = (a, b)^T$, namely,

$$\hat{\alpha} = \left(B^T B\right)^{-1} B^T Y_n. \quad (8)$$

Among

$$B = \begin{bmatrix} -z^{(1)} & (2) & 1 \\ -z^{(1)} & (3) & 1 \\ \vdots & & \\ -z^{(1)} & (n) & 1 \end{bmatrix}, \quad Y_n = \begin{bmatrix} x^{(0)} & (2) \\ x^{(0)} & (3) \\ \vdots & \\ x^{(0)} & (n) \end{bmatrix}, \quad (9)$$

$(dX^{(1)}/dt) + aX^{(1)} = b$ is called the whitening equation of the grey differential equation $x^{(0)}(k) + az^{(1)}(k) = b$, and the solution to the whitening equation is also called the event response function:

$$\hat{x}^{(1)}(t+1) = \left[x^{(1)}(0) - \frac{b}{a}\right]e^{-ak} + \frac{b}{a}, \quad k = 1, 2, 3, ..., n. \quad (10)$$

The corresponding time series of the GM (1, 1) grey differential equation $x^{(0)}(k) + az^{(1)}(k) = b$ is as follows:

$$\hat{x}^{(1)}(k+1) = \left[x^{(0)} - \frac{b}{a}\right]e^{-ak} + \frac{b}{a}, \quad k = 1, 2, 3, \ldots, n. \quad (11)$$

Taking $x^{(1)}(0) = x^{(0)}(1)$, calculate the simulate value $\hat{x}^{(1)}(k)$ of $X^{(1)}$.

By consecutive subtraction, the regression prediction value is as follows:

$$\hat{x}^{(0)}(k+1) = \hat{x}^{(1)}(k+1) - \hat{x}^{(1)}(k). \quad (12)$$

## 3. Pickup of First Signal Arrival Based on Entropy Method

A microseismic signal is composed of background noise and an effective signal. We can see from the time and frequency domains that the largest feature of the background noise is that it has a certain regularity in the macroregion and has large randomness at the microscopic level. Most existing methods, such as those using the amplitude, energy, or other factors, are at the microcosmic scale. Although the effect becomes clear at a particular moment in time, they are significantly affected by random noise and cannot be accurately identified when the amount of noise is too large. In this paper, the calculation of the signal entropy is used to describe the change in signal state from a macroscopic angle, and thus the interference caused by random noise is weakened. The introduction and application of entropy at the first arrival of a wave are realized through the following steps. There are three parts, namely, the division of the amplitude region, the selection of the rolling time window, and the entropy calculation.

*3.1. Regional Division.* The calculation of entropy is based on the frequency distribution of events that may occur. At present, microseismic monitoring equipment mostly includes speed and acceleration sensors, and the sampling frequency is discrete from 1 to 25 kHz and the sampling points. To calculate the frequency distribution of each region, we can divide the amplitude region artificially and then calculate the entropy value of the microseismic signal. For the width of the area division, the monitor scene should be considered. The width of the area is small, the pickup precision is high, and the operation time is long. In contrast, the accuracy of the pickup is low and the operation is faster. After testing, a range between zero and the maximum amplitude generally requiring 0–10 intervals is appropriate. In Figure 1, a vibration signal waveform, as shown in Figures 1(b) and 1(c), indicates the division of the amplitude regions.

*3.2. Time Window Selection.* To accurately pick up the first arrival of the signal and compare it with the traditional energy method, a rolling window suitable for the width is selected. The probability distribution of the signal in each region of the time window is calculated, as is the entropy value of the signal in the time window. The time window is selected as shown in Figure 2.

*3.3. Entropy Calculation.* In this paper, the entropy of the rolling window is calculated based on the means of information entropy and the change in statistical entropy:

$$H(X) = E\left[I(x_i)\right] = -\sum p_i \log p_i. \quad (13)$$

The $\sigma$ principle of statistics determines the first arrival time. For a normal distribution variable, the probability that its value falls within the range of $\overline{H} \pm 3\sigma$ is 0.9974, which is almost inevitable. Here, $\overline{H}$ and $3\sigma$ are the mathematical expectation and variance of the normal random variable, respectively. This method is equally applicable to the background noise. When there are no new signal sources, the change in entropy of the noise signal obeys a normal random variable. When a microseismic signal arrives at a certain time, the entropy will rapidly exceed 3 times the H variance of the original background noise, as shown in Figure 3. We believe that the small probability event is no longer the background noise, but the first arrival of the mine shock signal, that is, the first wave of the $P$ wave.

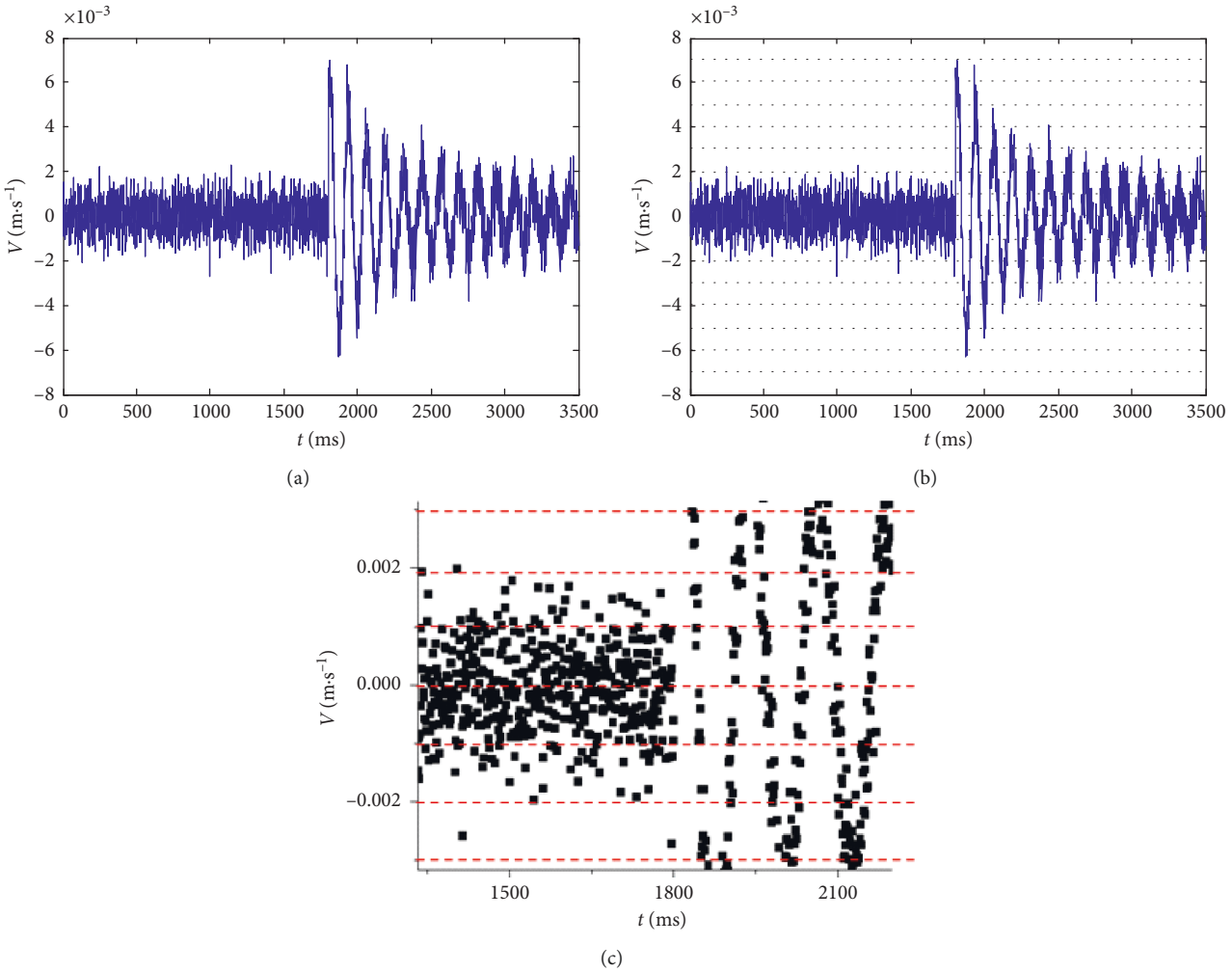


Figure 1: Region division of entropy method.

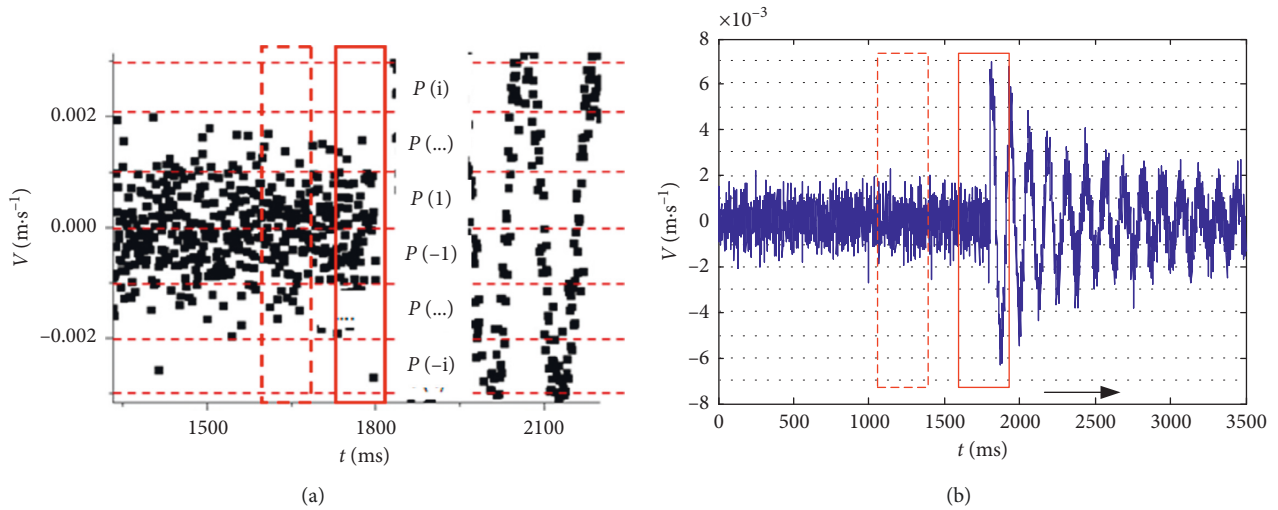


Figure 2: Time window selection of the entropy method.

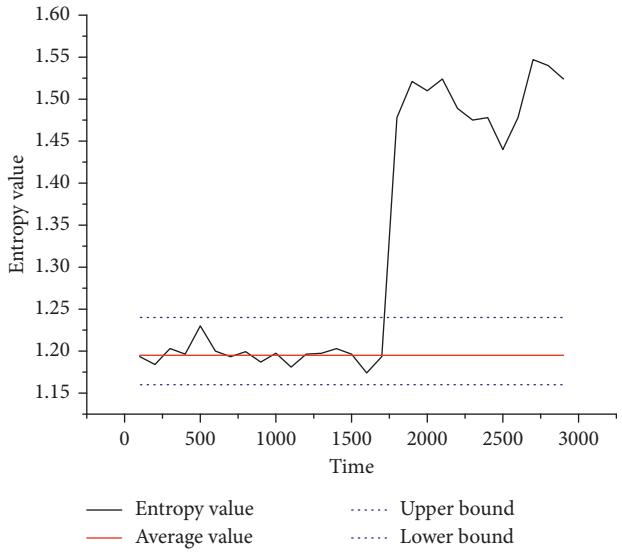


Figure 3: Entropy change of signal arrival.

As shown in Figure 2(b), the microseismic signal curve fluctuates less when the $P$ wave has not first arrived, and the curve fluctuates significantly between 1,500 and 2,000 ms. As shown in Figure 3, when the waveform curve is abrupt, which leads to a sudden change in the entropy value, the entropy curve also changes, and the moment of the mutation is the first arrival time of the $P$ wave.

## 4. Pickup Process of Signal's First Arrival Using Entropy Method

*4.1. Flow Chart of First Arrival Pickup Using Entropy Method.* The entropy method is used to pick up the first arrival of a signal, which is mainly divided into three parts, namely, the parameter selection, selection of the first arrival region, and the precise location. The detailed flow chart is shown in Figure 4.

*4.2. Parameter Selection.* The parameters of the first arrival pickup of the entropy method are mainly determined based on the lengths of four time windows. As shown in Figure 5, of these, 1 and 2 can fasten the position time window for the STA/LTA method, 3 is the time window of the entropy calculation, 4 is the grey prediction of the base value time window, and the time window lengths are set to $T_1$, $T_2$, $T_3$, and $T_4$.

*4.3. Area Determination of First Signal Arrival.* Because STA/LTA calculates the energy in the time window, it has the advantages of a strong resistance to impulse noise; however, its disadvantage is a poor pickup accuracy. Because the entropy calculation method has strong sensitivity to a signal change, an accidental noise pulse may affect the accuracy of the first arrival location. Taking into account the accelerating time of the pickup of the first arrival, we can use the STA/LTA method. First, a quick coarse picking location is applied. When the STA/LTA value is greater than the critical

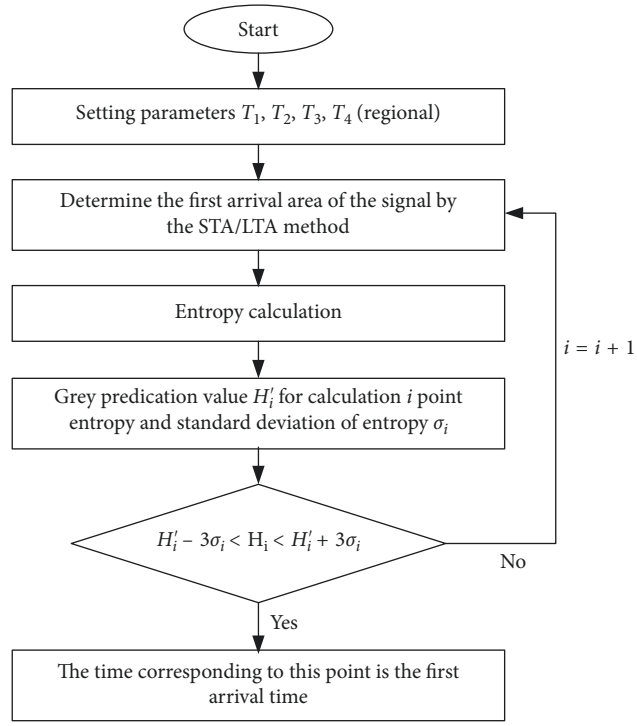


Figure 4: Flow chart of the entropy method.

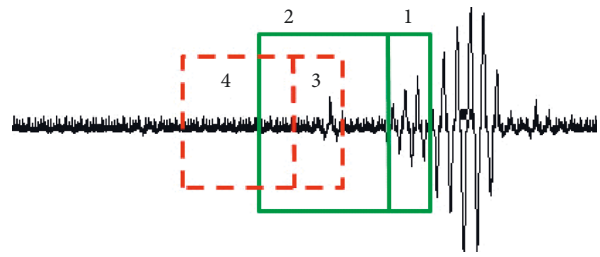


Figure 5: Time window of entropy method.

value $R$, windows 1 and 2 contain the first arrival area, the formula of which is

$$R = \frac{\sum_{t=T_0}^{T_2} x^2(t)}{\sum_{t=T_1}^{T_0} x^2(t)}, \tag{14}$$

where $x^2(t)$ is microseismic data, $T_0$ is the intersection of the short and long window times, $T_1$ is the beginning of the short window, and $T_2$ is the end time of the long window.

After the STA/LTA method, the approximate region of the first arrival of the signal can be preliminarily determined, and it can then be accurately positioned using the entropy method.

*4.4. Accurate Positioning*

*4.4.1. Entropy Calculation.* When the first arrival region is detected using the STA/LTA method, the entropy method is applied for an accurate pickup. After the entropy of point $i$ is calculated, the time window rolls downward. The entropy values of all points in the rough location of areas 1 and 2 are calculated sequentially, and the entropy value curves are plotted.

*4.4.2. Grey Prediction of Entropy.* Grey prediction is introduced during the first arrival pickup, and later it can make the first arrival pickup more accurate than a traditional method, taking into account the tendency of changes in noise. When setting the fast pickup area, there are $n+1$ points, $i$, $i+1$, $i+2$, ..., $i+n$, and the third time window contains $P$ points. The entropy value of window 3 is used as the first point of the fast pickup region, and the grey prediction basis value of $i$ points, the $i$ point predictive value $H_i'$, and standard deviation $\sigma_{\mathrm{i}}$ are obtained. Window 3 rolls down to a point, as the grey prediction basis value of the second $i+1$ point, the $i+1$ point prediction value $H_{i+1}'$, and the standard deviation $\sigma_{i+1}$ are obtained. This continues until the last point $i+q$, predictive value $H_{i+q}'$, and standard deviation $\sigma_{i+q}$ are calculated:

$$\sigma_i = \sqrt{\frac{\sum_{j=i-p}^{i-1}\left[x^{(0)}(j) - \overline{x}^{(0)}\right]^2}{p-1}}, \qquad \overline{x}^{(0)} = \frac{\sum_{i=i-p}^{i-1} x^{(0)}(k)}{p}. \tag{15}$$

*4.4.3. Determination of First Arrival Time.* Starting with the first point $i$, the actual $H_i$ and predicted values $H_i'$ of $i$ points are compared. If $H_i' - 3\sigma_i < H_i < H_i' + 3\sigma_i$ is not satisfied, the comparison of the next point $H_{i+1}$ is continued until point $i$ that satisfies the condition is found, and the time corresponding to the point is considered to be the first arrival time of the microseismic signal.

## 5. Sensitivity Analysis of First Signal Arrival Picking Method

By observing the change in the waveform of the signal before and after the first arrival, it can be seen that the waveform of the signal changes after the first arrival, mainly in terms of the amplitude, frequency, and seismic phase. In this paper, a synthetic signal is used to compare the entropy method with the practical Allen method and the fractal method.

A synthetic signal is used as the test signal, and 2,000 sampling points are used as the signals. Figure 6 shows an amplitude test signal, with 0–10 using a sine function with a maximum amplitude of 1 and 10–20 using a sine function with a maximum amplitude of 2. Figure 7 shows the amplitude frequency test signal, where the signal uses a sine function with a frequency of 1/2 within 0–10 s and a frequency of 1 within 10–20 s. Figure 8 shows the amplitude phase test signal, where the signal frequency is 1/2, and when the time is $10^+$, where the initial amplitude is $0^+$, and $10^-$ seconds, where the end of the amplitude is $0^+$.

*5.1. Allen Method.* Allen first proposed the concept of a characteristic function. When the wave arrives, the waveform, amplitude, and frequency are mutated, although the mutation is less pronounced. The characteristic

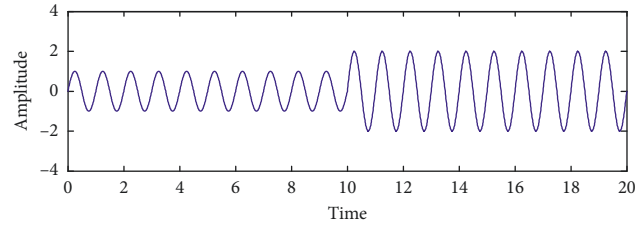


Figure 6: Analog signal of amplitude.

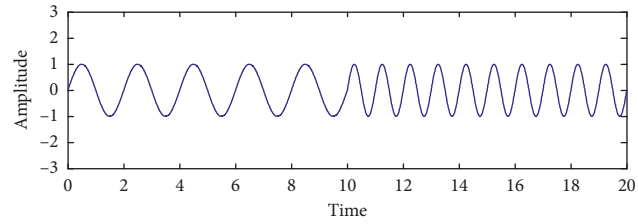


Figure 7: Analog signal of frequency.

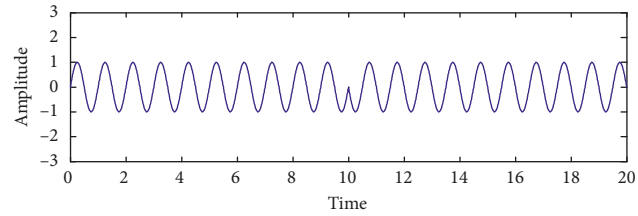


Figure 8: Analog signal of seismic phase.

function is used to calculate the waveform, and the first arrival time of the wave is amplified to provide the possibility for an accurate pickup. Let $X_i$ be the amplitude vector, that is, the time vector of the amplitude corresponding to the amplitude, and $X_i$ be the first-order difference of the amplitude; Allen defines an envelope function $E(t)$ as follows:

$$E(t) = x_i^2 + C_i \times \dot{x}_i^2, \tag{16}$$

where $C_i$ is the weight constant; that is, $C_i = \sum_j^i |x_j| / \sum_{j=1}^i |x_j - x_{j-1}|$.

We call $E(t)$ a characteristic function, and the Allen method is actually a development of the STA/LTA method. It mainly solves the disadvantage of the poor accuracy of the traditional STA/LTA method. The Allen method uses the method of constructing the characteristic function to find the abrupt point of the signal and then applies the ratio method to pick up the first arrival of the signal. Figure 9 shows the sensitivity of the simulation of the synthetic signal detection characteristic function to the waveform variations.

Figure 9 shows a sensitivity analysis of the amplitude of the Allen method. Before the amplitude changes, the characteristic function curve changes regularly. With the sudden increase in amplitude, the characteristic function also increases at an instant, and the characteristic function increases as well. Figure 10 shows a frequency sensitivity analysis of the Allen method. Before the change in

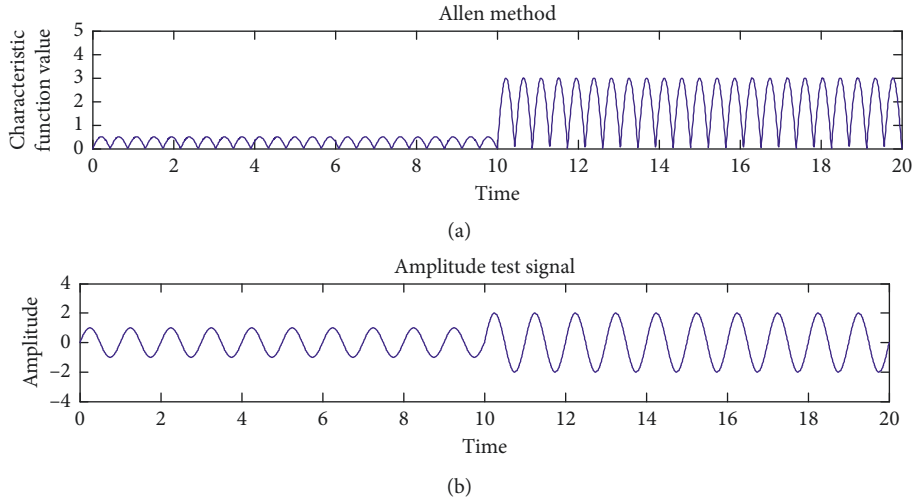


Figure 9: Amplitude sensitivity analysis of the Allen method.

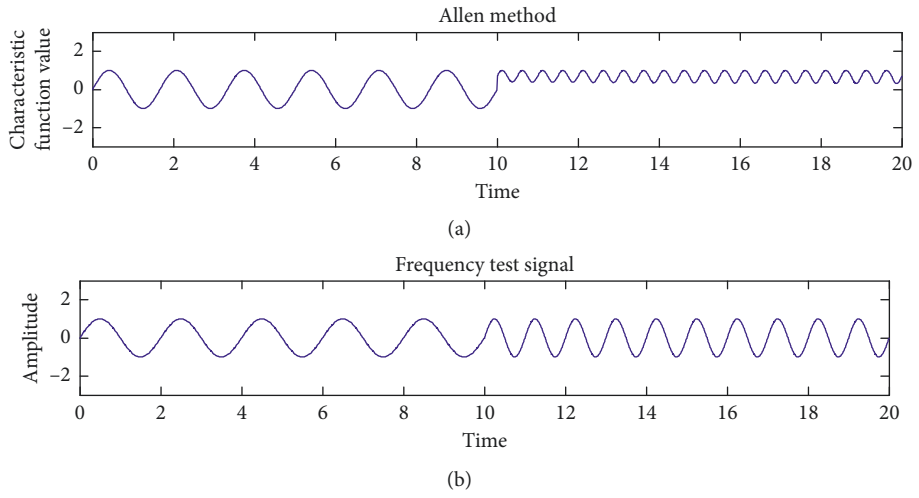


Figure 10: Frequency sensitivity analysis of the Allen method.

frequency, its characteristic function is similar to the sine law fluctuation. After the frequency changes, the characteristic function clearly changes, the vibration amplitude significantly decreases, and the frequency increases. Figure 11 shows the sensitivity analysis of the Allen seismic phase. Before the seismic phase changes, the characteristic functions all exhibit sinusoidal curves, with no obvious changes. As can be seen from Figures 9 and 10, the Allen method is sensitive to changes in amplitude and frequency, and the modified characteristic function can magnify the changes in amplitude, thereby facilitating the pickup. As can be seen from Figure 11, the Allen method is very insensitive to changes to the seismic phases, and there is no change in the characteristic curve, and thus the phase changes cannot be picked up at any moment.

*5.2. Fractal Method.* The calculation of a fractal dimension uses a box dimension calculation, and graphs can be expressed using the following equation:

$$D_s = \lim \frac{\ln N(\varepsilon)}{\ln(1/\varepsilon)}, \tag{17}$$

where $N(\varepsilon)$ is the total lattice number occupied by a curvilinear figure when the length of the side is $\varepsilon$.

The calculation method of the formula is aimed at a different side length $\varepsilon$. Here, $N(\varepsilon)$ and $\varepsilon$ are the logarithms used to make a straight-line fitting, and the slope is the fractal dimension. The first arrival of the wave based on the fractal method is also affected by the length of the time window. If it needs to be picked up accurately and quickly, it is necessary to adjust the length of the window according to the frequency of the different sampling points. The fractal rolling window is 40 sampling points, and the window is rolled in by the point-by-point manner.

Figure 12 shows amplitude sensitivity analysis of the fractal method. The fractal dimension exhibits periodic fluctuations before and after the amplitude changes, and there is no obvious change before or after such changes.

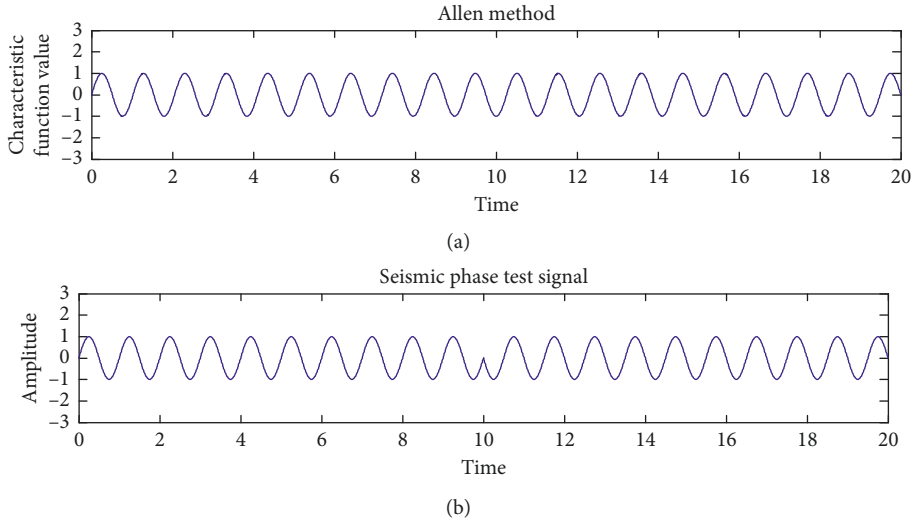


Figure 11: Seismic phase sensitivity analysis of the Allen method.

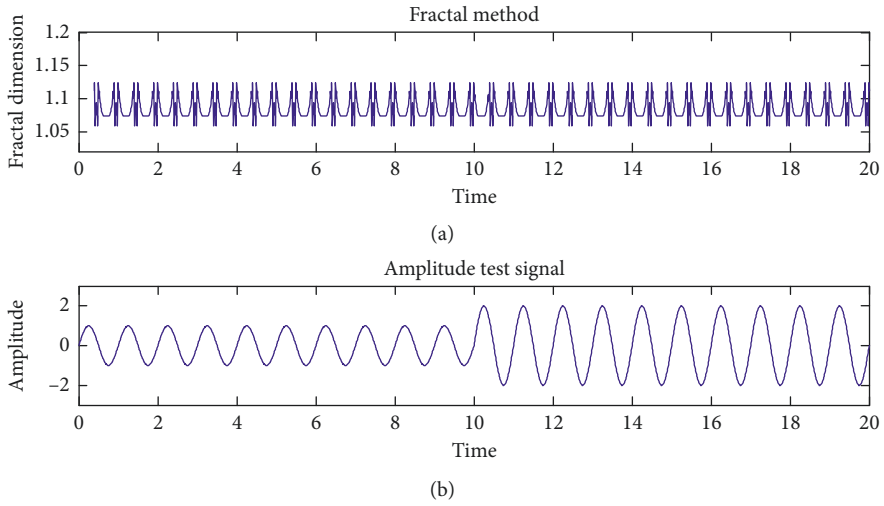


Figure 12: Amplitude sensitivity analysis of fractal method.

Figure 13 shows the sensitivity analysis of the fractal method to the frequency. It can be clearly seen that the fractal dimension changes regularly and periodically before the frequency changes. When the frequency changes, the amplitude of the fractal dimension clearly decreases, as does the change cycle. Figure 14 shows the sensitivity analysis of the fractal method to the frequencies and seismic phases. When the seismic phase changes, the fractal dimension increases and then gradually returns to normal, and the changes are therefore obvious. As can be seen from the three charts, the amplitude change is picked up based on the fractal method, which depends heavily on the choice of the time window length. The fractal method has very low sensitivity to amplitude changes and cannot pick up the change in moment effectively. When the frequency of the wave and seismic phase changes, the value of the fractal dimension will clearly change, providing the possibility of an accurate pickup.

*5.3. Entropy Method.* In this paper, the entropy method adopts information entropy, and the rolling time window of the entropy value is 80 sampling points, and the amplitude is divided into 10 regions, namely, (−2.5, −2), (−2, −1.5),(−1.5, −1), (−1, −0.5), (−0.5,0 ), (0, 0.5), (0.5, 1), (1, 1.5), (1.5, 2), and (2, 2.5). The probability of the sampling points in each region is calculated, and the entropy value curve is then obtained.

The entropy method detailed in this paper is used to describe the ordered or unordered state of a system. When the waveform state changes, the distribution of points in each interval will change, which will lead to a sudden change in entropy. Figure 15 shows an analysis of the entropy method of the amplitude sensitivity. It can be seen from the diagram that the entropy value of the information is smaller before the amplitude changes. At the moment of the amplitude change, the entropy curve is abrupt. An increase in amplitude leads to an increase in entropy, which is due to the

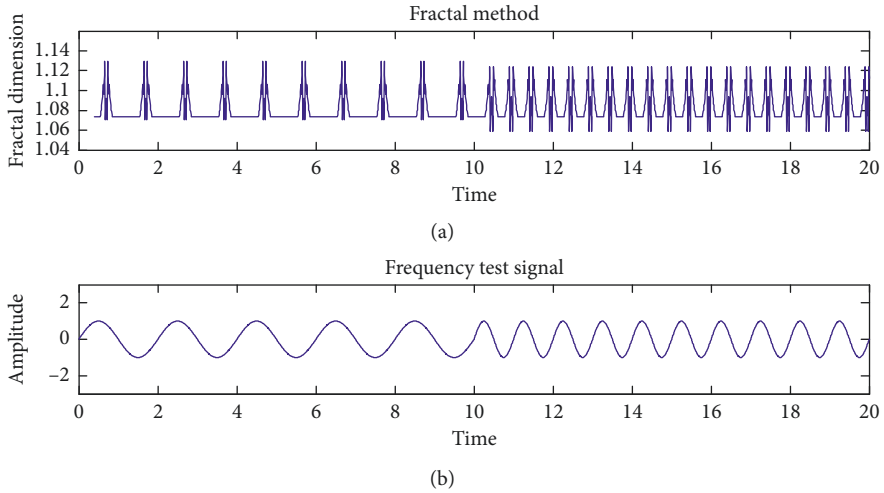


Figure 13: Frequency sensitivity analysis of fractal method.

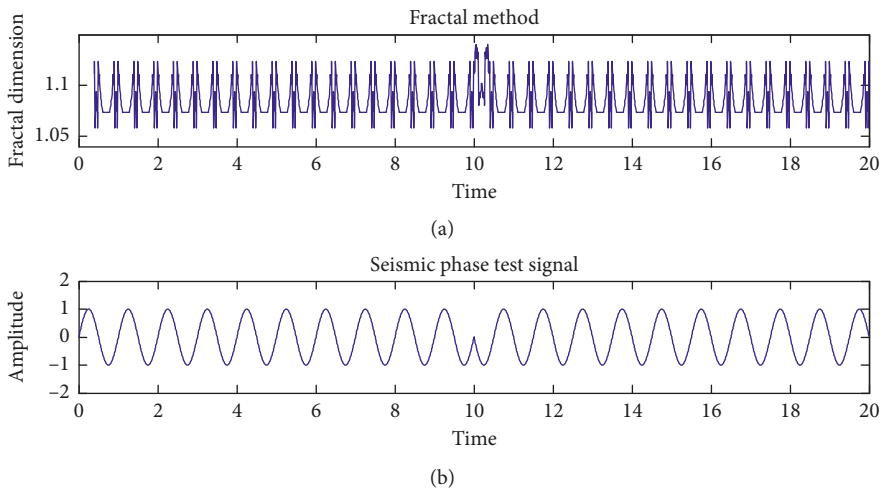


Figure 14: Seismic phase sensitivity analysis of fractal method.

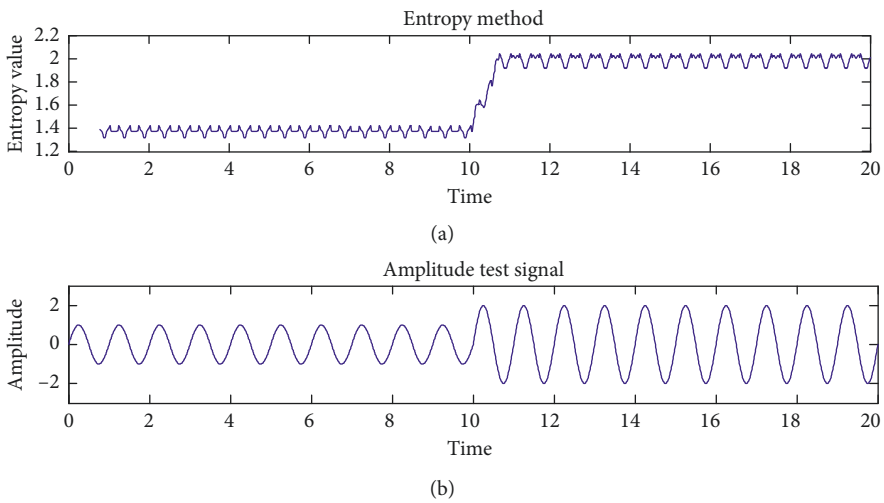


Figure 15: Amplitude sensitivity analysis of entropy method.

change in distribution of the sampling points in each interval of the calculation window. Figure 16 shows the frequency sensitivity analysis of the entropy method. At the moment of a frequency change, the entropy curve is abrupt. It can be seen that the entropy changes regularly and periodically before the frequency changes, and the fluctuation is large, whereas after the frequency changes, the entropy approximates to a constant. The reason for the occurrence of this phenomenon is related to the length of the time window selection. The length of the time window is fixed, and the time window does not contain a complete waveform before the frequency is changed. Therefore, the entropy curve produces an oscillation. After the frequency is changed, the time window contains the complete waveform and is thus close to a constant. When a larger length of the window is chosen, the entropy value tends to be a constant before the change, and a mutation occurs at the moment of change and then quickly returns to a constant. Figure 17 shows a seismic phase sensitivity analysis of the entropy method. Before the seismic phase changes, the entropy value is close to a constant and changes less. When the seismic phase change of the entropy value decreases rapidly, it returns the original value. When the phase changes, the entropy has a sudden change. The entropy value recovery is then due to the waveform phase change without affecting the amplitude and frequency, that is, the waveform is unchanged. It should be noted that the calculation of the entropy value in this paper has made improvements on the traditional calculation method of information entropy. Only the entropy value of the sampling points in the interval is calculated. Each time the window scrolls, the number of sampling points may be different. Therefore, it will not follow the rule in which the entropy value increases with an increase in the degree of chaos.

From the image obtained, compared with the Allen and fractal methods, the entropy method is extremely sensitive to changes in the amplitude, frequency, and seismic phase. The entropy value changes significantly before and after the change, which provides the possibility for the first arrival of the wave signal to be accurately picked up.

*5.4. Sensitivity Analysis of the First Arrival Pickup Method of Actual Microseismic Signals.* This paper selects the microseismic monitoring signal of the Jixian Coal Mine in Heilongjiang. The data acquisition equipment uses a multichannel high-frequency structure monitor and a signal sampling frequency of 10 kHz. As shown in Figure 18, the signal accurately determines the wave's first arrival time of 1,011 ms through a manual pickup. The Allen method, fractal method, and entropy method are used to pick up the first arrival time of the microseismic signal, and the sensitivity of the three methods to the first arrival of the microseismic signal is analyzed.

Figures 19–21 show comparisons of the first arrival time of signals picked up by the three methods, respectively. The results of the first arrival pickup of signals using the three methods are shown in Table 1. For the Allen method shown in Figure 19, the microseismic signal curve is stable before the first arrival of the signal, and the characteristic value curve peaks when the signal arrives. According to the result of the first signal arrival pickup, the Allen method easily picks up the first signal arrival, but its pickup precision is low. For the fractal method shown in Figure 20, the microseismic signal curve fluctuates slightly before the first arrival of the signal and fluctuates clearly when the signal arrives. Although the fractal method has a high pickup precision, it is difficult to determine the minimum fractal dimension value point of the first arrival time of the signal on the fractal dimension curve. For the entropy method shown in Figure 21, the microseismic signal curve fluctuates less before the signal arrives and fluctuates significantly when the signal first arrives. Between 1,000 and 1,500 ms, the waveform curve changes, which leads to a sudden change in the entropy value. The entropy value curve also mutates, and the point of a sudden change is the first arrival point of the signal. The entropy method easily picks up the first arrival point of the signal and has a high pickup accuracy.

Based on the Allen, fractal, and entropy methods, the results of the first arrival pickup of the signal are compared and analyzed. The results of the first arrival pickup using the entropy method are the closest to those by the manual method, and the change in the entropy value curve at the first arrival time is more obvious. The sensitivity of the entropy method to the first arrival moment of the signal is better than the other two methods.

## 6. Noise Immunity Analysis

As shown in Figure 22, this study selected the microseismic monitoring signal of the Jixian Coal Mine in Heilongjiang as the test signal, using a total of ten microseismic signals. Taking one of the blasting monitoring signals as an example, the remaining noise immunity results are listed in the tabular form. The sampling frequency is 10 kHz, based on a manual pickup, and the accurate time of the first arrival of the wave is 1,011 ms. White noise processing is applied using $y = \text{awgn}(x, \text{SNR})$, and we obtain a signal-to-noise ratio (SNR) of 20, 10, and 2 dB, respectively. The STA/LTA, fractal, and entropy methods are used to pick up the first arrival of the signal, and the noise immunity of the three methods is then compared. The results are shown in Table 2.

With the STA/LTA method, the long window time is 30 ms, the short window time is 5 ms, and $R = 1.4$, which is considered the beginning of the signal. With the fractal method, the time window uses points of 40 ms in length. With the entropy method, a short window time is 5 ms, the long window time is 30 ms, the grey prediction window time is 20 ms, the number of partitions $N = 6$, and the entropy value of the calculated time window is 40 ms. The best parameters determined after several attempts for comparison were applied. A positive value indicates a lag.

As can be seen from Table 2, the addition of noise can greatly affect the accuracy of the first arrival pickup. When

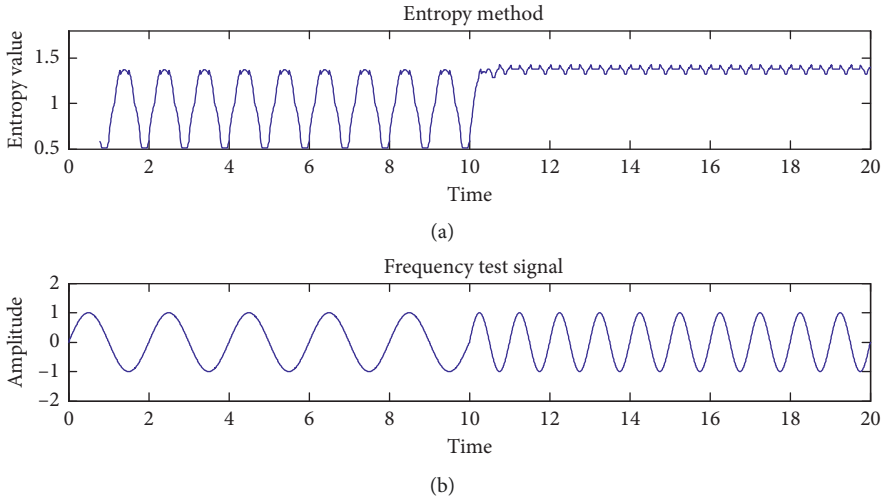


Figure 16: Frequency sensitivity analysis of entropy method.

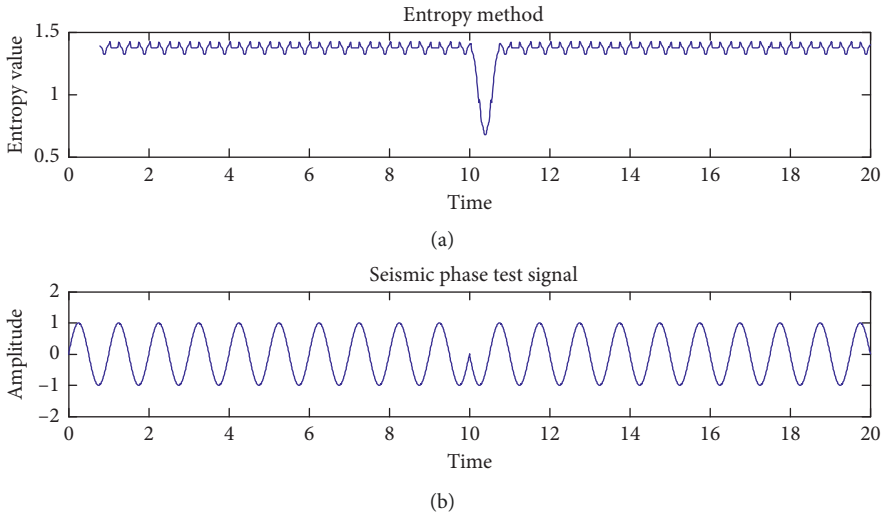


Figure 17: Seismic phase sensitivity analysis of entropy method.

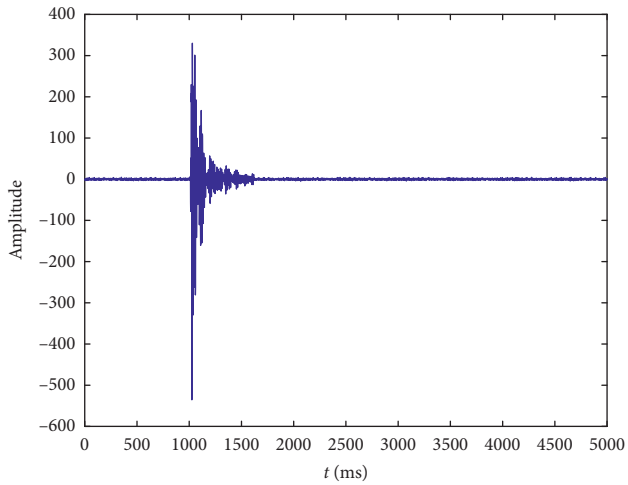


Figure 18: Second signal of 9:10:45–50 on May 7, 2018

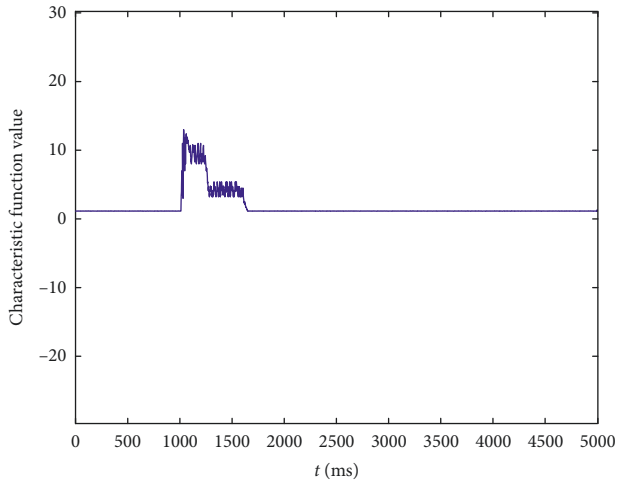


Figure 19: First signal arrival pickup sensitivity analysis of the Allen method.

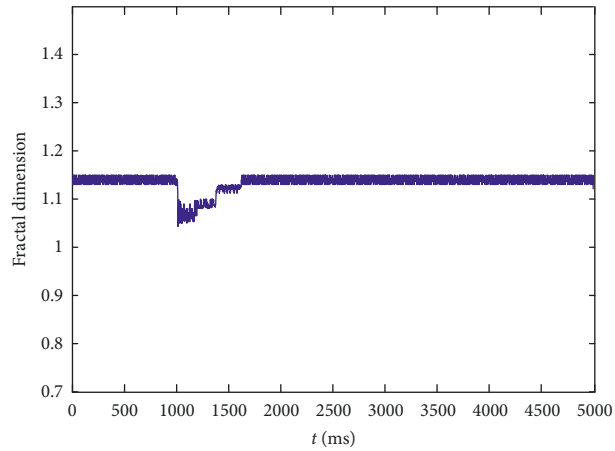


Figure 20: First signal arrival pickup sensitivity analysis of the fractal method.

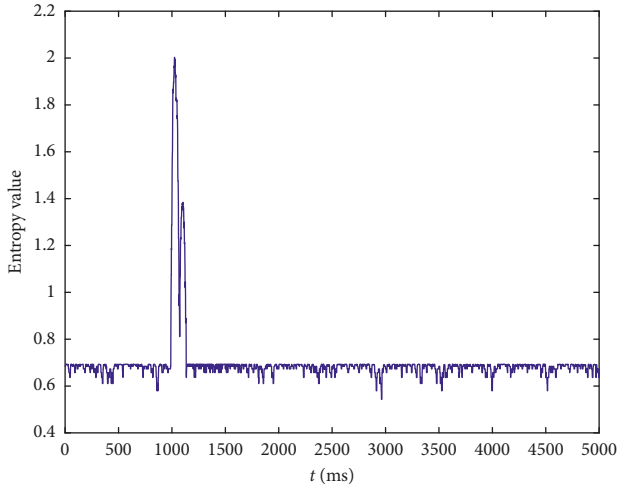


Figure 21: First signal arrival pickup sensitivity analysis of the entropy method.

Table 1: First signal arrival pickup results.

| Method | Allen method | Fractal method | Entropy method |
|---|---|---|---|
| First arrival time | 1012.2 ms | 1011.4 ms | 1011.3 ms |
| Picking error | 1.2 ms | 0.4 ms | 0.3 ms |

the SNR is no added noise, 20, 10, and 2 dB, the pickup error of STA/LTA is 1.1, 1.3, 1.4, and 4 ms, respectively. The pickup error of the fractal method is 0.3, 0.7, 1.1, and 2.9 ms, respectively. The pickup error of the entropy method is 0.3, 0.5, 0.9, and 1.9 ms, respectively. Table 3 shows the results of the pickup of nine other monitoring signals as compared with the three methods; the effect of the STA/LTA method is poor, whereas that of the fractal method has the second-best effect, and the entropy method achieves the best noise immunity.

## 7. Analysis of Influence of Calculation Parameters on the Pickup Error of the First Arrival

*7.1. Fractal Method.* When box dimensions are adopted, the pickup parameters have a fractal window length of $T$. Taking into account a $T$ of 20, 30, 40, 50, and 60 ms, the pickup error of the original signal is shown in Table 4. As can be seen from Figure 23, the fractal method has only one parameter $T$. When the $T$ value of the fractal window changes, it has a greater impact on the pickup error, and the trend in the variation first decreases and then increases. When $T = 40$ ms, the error reaches a minimum of 0.3 ms. The choice of $T$ values is not immutable and has a significant relationship with the waveform of the signal, and the selection of $T$ values of different types of waveform also differs.

*7.2. STA/LTA Method.* The pickup parameters of STA/LTA include a short time window of $T_1$, long time window of $T_2$, and critical value $R$. For convenience, regarding the influence of the time window selection on the pickup accuracy, $R$ takes a fixed value of 1.7. When the $T_1$ length is 5 and 10 ms and the $T_2$ length is 20, 30, 40, and 60 ms, the pickup error value is as shown in Table 5. When $T_1/T_2$ takes 5/20, 5/30, and 10/30 ms, and the $R$ value is 1.3, 1.5, 1.7, 1.9, and 2.1, respectively, and the picking error is as shown in Table 6.

As can be seen in Figure 24, the selection of $T_1$ and $T_2$ has a significant influence on the pickup error of the first signal arrival. When the short window time increases, the pickup error significantly increases, whereas the pickup efficiency increases. When the long window time increases, the pickup error increases.

Figure 25 shows the effects of the pickup error for different time window lengths and different $R$ values. As can be seen from the results, the short and long window times and the $R$ value have a significant influence on the results of the STA/LTA method. When $T_1$ and $T_2$ increase, the critical value $R$ changes accordingly, and the pickup error increases with an increase in the value of $R$. However, an overly high reduction in $R$ is not a good way to improve the accuracy, because the smaller the $R$ value is, the longer

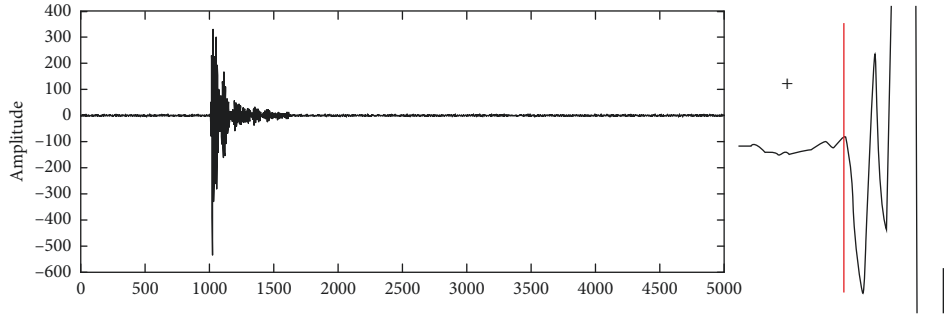


Figure 22: Test signal of microquake.

Table 2: Pickup time for different methods with different SNRs.

| Method | Signal-to-noise ratio | | | |
|---|---|---|---|---|
| | No added noise | 20 dB | 10 dB | 2 dB |
| STA/LTA method | 1012.1 | 1012.3 | 1013.4 | 1015.0 |
| Fractal method | 1011.3 | 1011.7 | 1012.1 | 1013.9 |
| Entropy method | 1011.3 | 1011.5 | 1011.9 | 1012.9 |

Table 3: Summary of the pickup time for different methods with different SNRs.

| Method | 1 | 2 | 3 | 4 | 5 | 6 | 7 | 8 | 9 |
|---|---|---|---|---|---|---|---|---|---|
| | | | | | No added noise | | | | |
| STA/LTA method | 1012.2 | 1012.4 | 1012.5 | 1012.3 | 1012.2 | 1012.1 | 1012.0 | 1012.4 | 1012.2 |
| Fractal method | 1011.3 | 1011.4 | 1011.5 | 1011.4 | 1011.3 | 1011.4 | 1011.4 | 1011.5 | 1011.3 |
| Entropy method | 1011.2 | 1011.3 | 1011.4 | 1011.3 | 1011.2 | 1011.3 | 1011.4 | 1011.4 | 1011.3 |
| | | | | | Added noise of 20 dB | | | | |
| STA/LTA method | 1012.4 | 1012.6 | 1012.7 | 1012.5 | 1012.4 | 1012.3 | 1012.2 | 1012.6 | 1012.4 |
| Fractal method | 1011.5 | 1011.6 | 1011.8 | 1011.8 | 1011.5 | 1011.7 | 1011.5 | 1011.9 | 1011.5 |
| Entropy method | 1011.4 | 1011.5 | 1011.6 | 1011.5 | 1011.4 | 1011.5 | 1011.4 | 1011.6 | 1011.4 |
| | | | | | Added noise of 10 dB | | | | |
| STA/LTA method | 1013.5 | 1013.6 | 1013.7 | 1013.5 | 1013.4 | 1013.3 | 1013.2 | 1013.6 | 1013.4 |
| Fractal method | 1012.2 | 1012.3 | 1012.4 | 1012.7 | 1012.1 | 1012.4 | 1012.0 | 1012.4 | 1012.1 |
| Entropy method | 1012.0 | 1012.1 | 1012.1 | 1011.9 | 1011.8 | 1011.8 | 1011.7 | 1011.9 | 1011.7 |
| | | | | | Added noise of 2 dB | | | | |
| STA/LTA method | 1015.1 | 1015.2 | 1015.4 | 1015.1 | 1015.0 | 1014.9 | 1014.8 | 1015.2 | 1015.0 |
| Fractal method | 1013.9 | 1014.0 | 1014.2 | 1013.8 | 1013.7 | 1013.4 | 1013.2 | 1013.9 | 1013.6 |
| Entropy method | 1012.9 | 1012.9 | 1013.0 | 1012.7 | 1012.7 | 1012.6 | 1012.3 | 1012.9 | 1012.7 |

Table 4: Influence of parameter selection on error of the fractal method.

| | Window $T$ | | | | |
|---|---|---|---|---|---|
| | 20 ms | 30 ms | 40 ms | 50 ms | 60 ms |
| Picking error | 1.9 | 0.7 | 0.3 | 0.3 | 0.9 |

the computation length, and a phenomenon in which the pickup sensitivity is increased occurs, causing a false judgment.

*7.3. Entropy Method.* In this paper, the entropy method has a plurality of pickup parameters. Among them, $T_1$ and $T_2$ are the fast positioning time windows for the STA/LTA method, $R$ is the critical value of the fast energy ratio method, $T_3$ is the time window for the entropy value, $T_4$ is the base time window of the grey prediction value, and $N$ is the subarea of the entropy value calculation. When the original signal without noise is used and when manually picking up the signal's arrival time within 1,011 ms, the values of $T_1$, $T_2$, $T_3$, and $T_4$ are 5, 40, 30, and 20 ms, respectively, $R$ takes a value of 1.7, and $N$ has six partitions. The influence of each parameter change on the pickup error is investigated.

Figure 26(a) is a change diagram of the pickup error when $T_1$ takes 5, 10, 25, 15, and 20 ms. Figure 26(b) shows a change diagram of the pickup error when $T_2$ takes 30, 40, 50, and 60 ms. Figure 26(c) shows a change diagram of the pickup error when $T_3$ takes 10, 20, 30, 40, 50, 60, 70, and

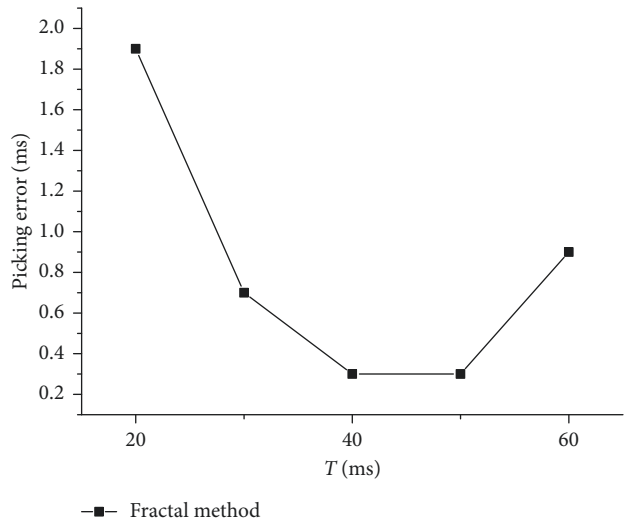


Figure 23: The influence of parameter selection on error of fractal.

Table 5: Pickup time error of different parameters when $R = 1.7$

| | $T_2$ | | | |
|---|---|---|---|---|
| $T_1$ | 20 ms | 30 ms | 40 ms | 60 ms |
| 5 ms | 1.3 | 1.1 | 1.8 | 4.2 |
| 10 ms | 1.6 | 1.4 | 1.2 | 3.5 |
| 15 ms | 2.1 | 1.6 | 1.3 | 1.2 |

Table 6: Pickup time error of different values of $R$.

| | $R$ | | | |
|---|---|---|---|---|
| STA/LTA | 1.3 | 1.5 | 1.7 | 1.9 |
| 5/20 ms | 1.1 | 1.4 | 1.7 | 2.3 |
| 5/30 ms | 1.2 | 1.5 | 2.0 | 2.6 |
| 10/30 ms | 1.1 | 1.3 | 1.4 | 1.9 |

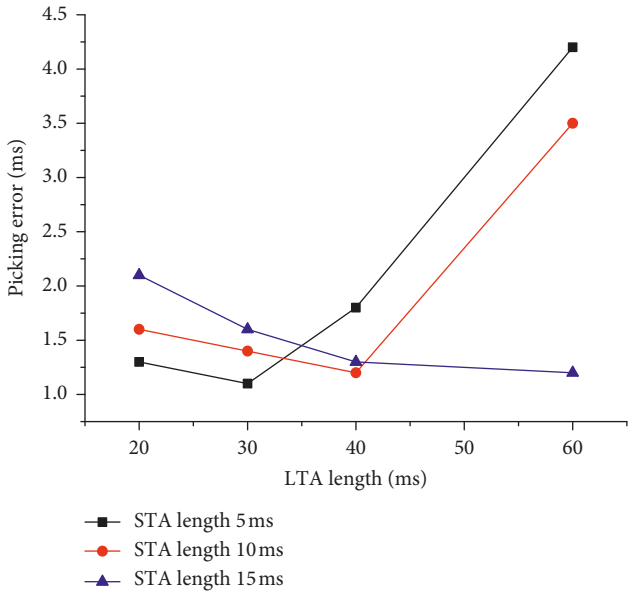


Figure 24: Pickup time error of different parameters when $R = 1.7$.

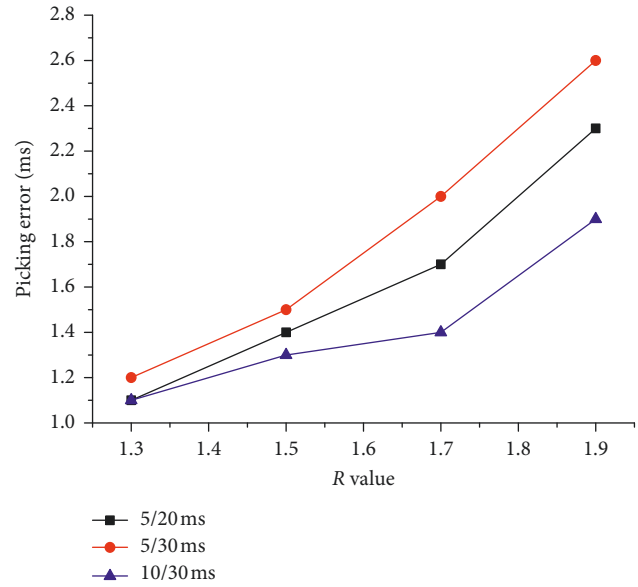


Figure 25: Pickup time error of different values of $R$.

80 ms. Figure 26(d) shows a change diagram of the pickup error when $T_4$ takes 10, 20, 30, 40, and 50 ms. Figure 26(e) shows a change diagram of the pickup error for $R$ of 1.4, 1.6, 1.8, 2.2, and 2.5. Figure 26(f) shows a change diagram of the pickup error for $N$ of 4, 6, 8, 10, 12, 14, and 16. From Figures 26(a), 26(b), and 26(e), it can be seen that the change in $T_1$, $T_2$, and $R$ does not affect the pickup accuracy because a fast pickup is only a preliminary positioning. Its function is to make the pickup faster and eliminate the impact of accidental pulse signals on the pickup accuracy. When the location is completed, the location region will be picked up again by the entropy method, and the change of its value has no influence on the pickup accuracy. As shown in Figure 26(d), the change in $T_4$ has an influence on the pickup accuracy, although the degree of influence is quite small. Because $T_4$ is the grey prediction window, its length affects the grey prediction database. When the length is large, by taking more points, the prediction results are more prone to outdated data. When the length is short and fewer points are taken, the prediction value depends on the new data. Figure 26(f) shows that when the number of partitions $N$ is 4, it has a greater impact on the pickup, and when $N$ increases to 8, the impact on the pickup accuracy decreases rapidly to zero. After many tests, for a general $T_4$ value of 10 to 30 ms, an $N$ of 8 is more appropriate. Generally speaking, although there are many parameters used in this method, a large number have little to no influence on the pickup accuracy, and the method is stable.

## 8. Conclusion

In this paper, both traditional and new methods for determining the first arrival pickup of microseismic signals were introduced. The new method is called the entropy method. The new and traditional methods were comparatively analyzed in terms of their sensitivity, signal pickup,

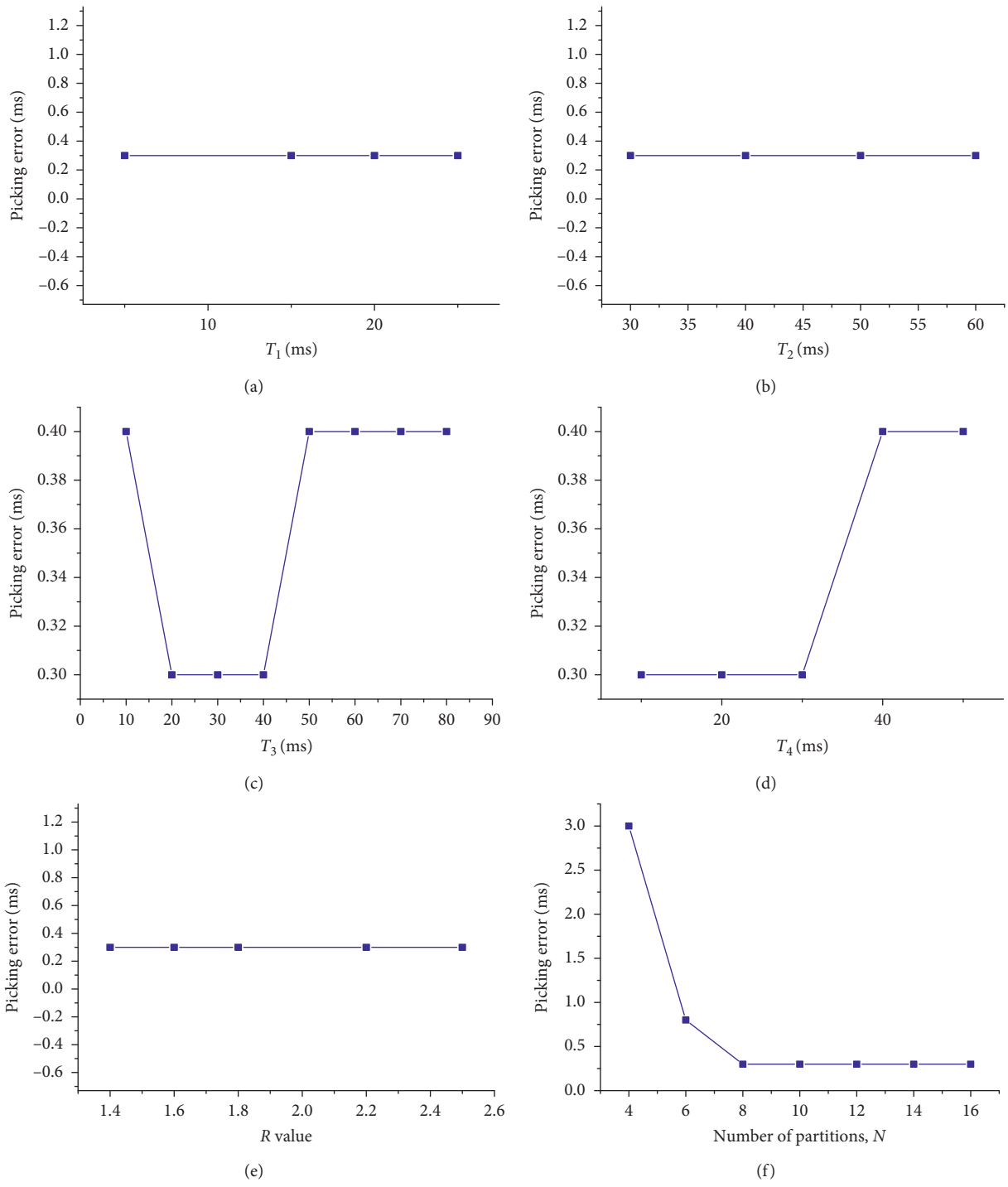


Figure 26: Influence of parameter selection on the error of the entropy method.

and antinoise capability under the influence of errors. The following results were obtained:

(1) The sensitivity of the amplitude, frequency, and seismic phase change of the Allen method were compared with the fractal and entropy methods based on synthesizing signals. The results show that the sensitivity of the Allen method to amplitude and frequency is higher, and a change in the characteristic function can be clearly seen. However, the sensitivity to a seismic phase change is weak, and the characteristic function has no clear change. The change in frequency and seismic phase by the fractal method is clear, but its sensitivity to the amplitude is poor, with almost no change. The entropy method has a higher sensitivity to changes in amplitude, frequency, and seismic phase and is therefore convenient for picking up the moment of change.

(2) By adding white noise through microseismic signals, different SNRs were obtained. The noise resistance of the STA/LTA, fractal, and entropy methods were compared and analyzed. The results show that the entropy method has better noise immunity, followed by the fractal method, whereas the STA/LTA method has poor noise immunity.

(3) The influence of the parameters on the pickup accuracy of the three methods was analyzed. The results show that the STA/LTA method has a stronger dependence on the length of the time window and the critical $R$ value and that the maximum error is 4 ms. The fractal method has less dependence on the length of the time window, and the maximum error is 1.9 ms. The entropy method has more parameters, but some have no influence on the pickup accuracy, and only the $N$ value has a greater impact. However, when the value of $N$ is larger than 8, the influence is significantly reduced, reaching close to zero, and the error is only 0.4 ms.

## Data Availability

The data used to support the findings of this study are available from the corresponding author upon request.

## Conflicts of Interest

The authors declare that there are no conflicts of interest regarding the publication of this paper.

## Acknowledgments

This work was supported by the National Natural Science Foundation of China (grant no. 51774173) and the Natural Science Foundation of Liaoning Province, China (grant no. 201602351). The authors would like to express their gratitude to all those who helped in writing this thesis. First, the authors are grateful for use of the site and the technical support of the manager and technical staff of the Heilongjiang Jixian Coal Mine. Second, they would like to thank the postgraduates of Liaoning Technical University for their help in the experiments. Lastly, the authors would like to thank Editage (https://www.editage.cn) for the English language editing.

## References

[1] Y. Jiang, Y. Pan, F. Jiang et al., "State of the art review on mechanism and prevention of coal bumps in China," *Journal of China Coal Society*, vol. 39, no. 2, pp. 205–213, 2014.

[2] Y. Jiang and Y. Zhao, "State of the art: investigation on mechanism, forecast and control of coal bumps in China," *Chinese Journal of Rock Mechanics and Engineering*, vol. 34, no. 11, pp. 2188–2204, 2015.

[3] Z. Bian, H. I. Inyang, J. L. Daniels, F. Otto, and S. Struthers, "Environmental issues from coal mining and their solutions," *Mining Science and Technology (China)*, vol. 20, no. 2, pp. 215–223, 2010.

[4] R. G. Jarrett, "A note on the intervals between coal-mining disasters," *Biometrika*, vol. 66, no. 1, pp. 191–193, 1979.

[5] Li Nan, E. Wang, and G. Maochen, "Microseismic monitoring technique and its applications at coal mines present status and future prospects," *Journal of China Coal Society*, vol. 42, no. 1, pp. 83–96, 2017.

[6] F. Jiang, G. Ye, C. Wang et al., "Application of high-precision microseismic monitoring technique to water inrush monitoring in coal mine," *Chinese Journal of Rock Mechanics and Engineering*, vol. 27, no. 9, pp. 1932–1938, 2008.

[7] B. Yu, J. Zhao, and H. Xiao, "Case study on overburden fracturing during long wall top coal caving using microseismic monitoring," *Rock Mechanics and Rock Engineering*, vol. 50, no. 2, pp. 507–511, 2017.

[8] N. Xu, C. Tang, H. Li et al., "Excavation-induced microseismicity: microseismic monitoring and numerical simulation," *Journal of Zhejiang University Science A*, vol. 13, no. 6, pp. 445–460, 2012.

[9] G. Zuo, Y. Wang, and R. Sui, "An improved method for first arrival pick up using energy ratio," *Geophysical Prospecting for Petroleum*, vol. 43, no. 4, pp. 345–347, 2003.

[10] H. Akaike, "Information theory and an extension of the maximum likelihood principle," in *Proceedings of 2nd International Symposium on Information Theory*, pp. 267–281, Akademiai Kiado, Budapest, Hungary, September 1973.

[11] H. Zhang, G. Zhu, and Y. Wang, "Automatic microseimic event detection and picking method," *Geophysical and Geochemical Exploration*, vol. 37, no. 2, pp. 269–273, 2013.

[12] R. V. Allen, "Automatic earthquake recognition and timing from single traces," *Bulletin of the Seismological Society of America*, vol. 68, no. 5, pp. 1521–1532, 1978.

[13] R. V. Allen, "Automatic phase pickers: their present use and future prospects," *Bulletin of the Seismological Society of America*, vol. 72, no. 6, pp. 225–242, 1982.

[14] J. Liu, Y. Wang, and Z. Yao, "On microseismic first arrival identification: a case study," *Chinese Journal of Geophysics*, vol. 56, no. 5, pp. 1660–1666, 2013.

[15] B. Jia, M. Jiang, and P. Zhao, "Seismic phase arrival time identification methods of mine earthquake and its application based on fractal theory," *Journal of Liaoning Technical University: Natural Science*, vol. 34, no. 10, pp. 1125–1130, 2015.

[16] R. Jia, Y. Tan, H. Sun et al., "Method of automatic detection on microseismic P arrival time under low signal to noise ratio," *Journal of China Coal Society*, vol. 40, no. 8, pp. 1845–1852, 2015.

[17] Y. Tan, J. Yu, G. Feng et al., "Arrival picking of microseismic events using the SLPEA algorithm," *Chinese Journal of Geophysics*, vol. 59, no. 1, pp. 185–196, 2016.

[18] R. Sharma, R. Pachori, and U. Acharya, "Application of entropy measures on intrinsic mode functions for the automated identification of focal electroencephalogram signals," *Entropy*, vol. 17, no. 2, pp. 669–691, 2015.

[19] J. Ródenas, M. García, R. Alcaraz, and J. Rieta, "Wavelet entropy automatically detects episodes of atrial fibrillation from single-lead electrocardiograms," *Entropy*, vol. 17, no. 12, pp. 6179–6199, 2015.

[20] A. Ramírez-Rojas, E. Flores-Márquez, N. Sarlis, and P. Varotsos, "The complexity measures associated with the fluctuations of the entropy in natural time before the deadly México M8.2 earthquake on 7 September 2017," *Entropy*, vol. 20, no. 6, p. 477, 2018.

[21] I. Zoukaneri and M. J. Porsani, "A combined wigner-ville and maximum entropy method for high-resolution time

frequency analysis of seismic data," *Geophysics*, vol. 80, no. 6, pp. O1–O11, 2015.

[22] J. Deng, X.-B. LI, and G. U. De-sheng, "Probability distribution of rock mechanics parameters by using maximum entropy method," *Chinese Journal of Rock Mechanics and Engineering*, vol. 23, no. 13, pp. 2177–2181, 2004.

[23] A. Abbas, A. H. Cadenbach, and E. Salimi, "A Kullback–Leibler view of maximum entropy and maximum log-probability methods," *Entropy*, vol. 19, no. 5, p. 232, 2017.